Geometric description of chaos in self-gravitating systems

Monica Cerruti-Sola[1] and Marco Pettini[1,2]
[1]*Osservatorio Astrofisico di Arcetri, Largo Enrico Fermi 5, 50125 Firenze, Italy*
[2]*Istituto Nazionale di Fisica Nucleare, Sezione di Firenze, Largo Enrico Fermi 2, 50125 Firenze, Italy*
(Received 1 June 1994)

This paper tackles the problem of the origin of dynamic chaos in Hamiltonian systems, with a special emphasis on the self-gravitating N-body systems. A Riemannian approach is adopted. The relationship between dynamic instability and curvature properties of the configuration space manifold is the main concern of this paper. Dynamic instability is studied with the aid of the Jacobi–Levi-Civita (JLC) equation for the geodesic spread. We point out that the approximations introduced so far to make the JLC equation handy, that is, to obtain a scalar equation describing the dynamical instability, are still too severe. In order to assess the validity limits of these approximations, the aid of numerical simulations is essential. For this reason, our analysis is supported by the numerical study of the dynamics of 10 and 100 gravitationally interacting point masses. The self-gravitating N-body systems provide an illuminating example of the relevant difference between geodesic flows of abstract ergodic theory and geodesic flows of physical interest. In fact, even though they correspond to manifolds of almost everywhere negative scalar curvature, this does not determine by itself the degree of chaos of these systems. We show that the quantities determining the instability of nearby trajectories do not simply coincide with scalar or Ricci curvature; rather they involve also other ingredients that are ultimately responsible for the existence of two different mechanisms to make chaos. The quantities mentioned enter a Hill equation and give instability either when they are negative or—when positive—because of parametric resonance. From numerical computations the ϵ (energy density) dependence of the dynamic instability exponents is found to be $\sim\epsilon^{3/2}$. Our paper aims at warning about the possibility of misleading conclusions that might be drawn from the geometric approach if the existence of the problems discussed here is ignored. Finally, we briefly discuss the relationship of the Riemannian geometric description of chaos with Lyapunov exponents in the special case of gravitational N-body systems.

PACS number(s): 05.45.+b, 95.10.Ce, 95.10.Fh

I. INTRODUCTION

The present paper is a continuation along the line of a recently proposed differential geometrical approach to Hamiltonian chaos [1,2]. This is based on the possibility of formulating Newtonian dynamics in terms of Riemannian geometry and then exploiting standard mathematical tools to provide a new explanation of the origin of chaos in a broad class of systems of physical interest. The idea is not completely new. It dates back to the pioneering work of Krylov on the foundations of statistical mechanics in connection with a dynamic explanation of phase space mixing [3]. Geodesic flows on Riemannian manifolds are also used in abstract ergodic theory [4]. In a Riemannian framework there are also few works aiming at demonstrating ergodicity or strong chaos in more physical systems [5,6] and other works of, say, heuristic nature, concerning the problem of collective relaxation and mixing in gravitational N-body systems [7–10].

What is new in the approach proposed in Refs. [1,2] is the idea that geometry must enfold all the information concerning regularity and weak or strong chaos of dynamics and that this can be directly checked by numerical simulations. The latter is a key point. In fact, the only possibility of working out good mathematical results is limited, roughly speaking, to manifolds of constant negative curvature, but this is not the general case of Hamiltonian flows of physics. Actually, numerical simulations led to the discovery of a new mechanism to make chaos: parametric resonance due to positive curvature fluctuations along geodesics. This circumstance opens new perspectives and problems for a Riemannian theory of Hamiltonian chaos.

In a very recent work [11] dealing with two degrees of freedom Hamiltonians, we have used the exact Jacobi–Levi-Civita (JLC) equation for geodesic spread to show in great detail that both the qualitative and quantitative information about order and chaos are contained in the solutions of the JLC equation. By qualitative information we refer to what is usually obtained with Poincaré surfaces of section and by quantitative information to that given by the Lyapunov characteristic exponent. This is a good point to make reasonable the claim that geometry must enfold all the properties of dynamics. However, when the number of degrees of freedom is large, one is compelled to use approximate versions of the JLC equation; the present paper aims at discussing in some detail the consequences of the natural approximations introduced so far, as well as to show what kind of loss of information is also implied.

In Sec. II we recall the basic definitions and concepts of the geometric description of chaos, and then the approximations of the JLC equation are discussed. In Sec.

III some numerical results concerning the gravitational N-body problem are given to show that the relationship between chaos and Riemannian curvature is subtler than might be suspected. In the light of our present approach to the description of chaos, we also comment about the meaning of Lyapunov exponents for the self-gravitating systems.

II. RIEMANNIAN DESCRIPTION OF CHAOS

Let us briefly recall some major points concerning the geometrical description of Newtonian dynamics. We consider conservative systems described by Hamiltonian functions such as

$$H(\mathbf{p},\mathbf{q})=\sum_{i=1}^{\mathcal{N}}\tfrac{1}{2}p_i^2+V(\mathbf{q}) \tag{1}$$

or, equivalently, by the Lagrangian

$$L(\dot{\mathbf{q}},\mathbf{q})=\sum_{i=1}^{\mathcal{N}}\tfrac{1}{2}\dot{q}_i^2-V(\mathbf{q})\ . \tag{2}$$

A large number of physical systems are described by such functions; $\mathcal{N}$ is the total number of degrees of freedom.

The natural motions described by the Lagrangian (2) are, among all the varied synchronous paths with initial and final configurations held fixed, those fulfilling the condition

$$\delta\int_{t_0}^{t_1}L(q^i,\dot{q}^i)dt=0\ , \tag{3}$$

which is Hamilton's least action principle. There are many equivalent formulations of this principle. Among them the so-called Maupertuis least action principle is our starting point; it states that the trajectories of a mechanical system are given by the condition

$$\delta\int_{\gamma(t)}2T(q^i,\dot{q}^i)dt=0\ , \tag{4}$$

where T is the kinetic energy and $\gamma(t)$ are all the isoenergetic curves joining two given points $\mathbf{q}_0$ and $\mathbf{q}_1$.

Now, remember that, given two points A and B on a Riemannian manifold, among all the possible paths joining them, a geodesic line is such that the arc-length functional is stationary, i.e.,

$$\delta\int_A^B ds=0\ . \tag{5}$$

Locally this also means that a geodesic is the shortest path between A and B.

By comparing (4) and (5) we realize how the geometrization of Newtonian dynamics is possible. In fact, by setting $ds=\sqrt{2}T(q^i,\dot{q}^i)dt$, $A\equiv\mathbf{q}_0$, and $B\equiv\mathbf{q}_1$, configuration space M is given the structure of a proper Riemannian manifold. Thus the trajectories of a mechanical system can be viewed as geodesics of the configuration space manifold if this is equipped with the kinetic energy metric.

The kinetic energy metric tensor of M is defined through

$$ds^2=g_{ik}(\mathbf{q})dq^i dq^k=2[E-V(\mathbf{q})]a_{ik}dq^i dq^k\ , \tag{6}$$

where E is the total energy and a_{ik} is the kinetic energy metric associated with the free Lagrangian ($V=0$), i.e., such that $2T(\dot{\mathbf{q}},\mathbf{q})=a_{ik}\dot{q}^i\dot{q}^k$. In Cartesian coordinates it is $a_{ik}=\delta_{ik}$. Equation (6) tells us that the metric tensor g_{ik} in the presence of a potential function V is obtained by a conformal transformation of a_{ik}; in order to have a nonsingular metric a restriction is needed to those configurations of the system such that $E>V(\mathbf{q})$ (E is the energy).

In local coordinates, the geodesic equations are

$$\frac{d^2q^i}{ds^2}+\Gamma^i_{jk}\frac{dq^j}{ds}\frac{dq^k}{ds}=0\ , \tag{7}$$

where s is the proper time and Γ^i_{jk} are the Christoffel coefficients of the Levi-Civita connection associated with g_{ik}. Using $g_{ik}=[E-V(\mathbf{q})]\delta_{ik}$, defining $W=E-V(q^a)$, and since $ds^2=2W^2dt^2$, from Eq. (7) one gets

$$\frac{d^2q^i}{dt^2}=-\frac{\partial V}{\partial q^i}\ , \tag{8}$$

i.e., Newton equations.

Let us now briefly discuss the relationship between the stability of the geodesics of a Riemannian manifold and the curvature properties of the same manifold. This is necessary to develop a geometrical point of view about the dynamical stability properties of natural motions described by (8).

The link between stability and curvature is given by the second-order variations of the arc-length functional or, equivalently, of the action functional. In fact, a geodesic and a mechanical motion must obey (7) and (8), respectively, in order to ensure a vanishing first-order variation of the functionals in (4) and (5). However, Eqs. (4) and (5) alone cannot determine whether these functionals attain a maximum or a minimum; this can be understood only if second-order variations are considered. We can intuitively grasp that if a geodesic (and so its corresponding mechanical motion) makes stationary the arc-length (action) functional without minimizing it, then it will be unstable with respect to variations—even small—of the initial conditions.

Instability of nearby trajectories leads to *chaos* under two circumstances: (i) the instability condition has to hold true for an appreciable measure of initial conditions in phase space, i.e., there must be a finite probability for the phase trajectories to encounter such regions of instability after a finite recurrence time, and (ii) the configuration space manifold (M,g_J) must be compact, i.e., the coordinates have to remain bounded during their time evolution. In fact, there are two basic ingredients in order to make a deterministic dynamics chaotic: *stretching* and *folding* of phase space volumes [12]. In the Riemannian description of Hamiltonian chaos, *stretching* of nearby trajectories is provided by *instability* and *folding* by not allowing the distance between trajectories to grow indefinitely, that is, by compactness of the ambient manifold. With these conditions, the phase trajectories are compelled to fold themselves in a very complicated fashion, which makes them forget the initial conditions

and makes their evolution practically unpredictable (at least for times sufficiently greater than the instability time scale). This way of looking at the origin of Hamiltonian chaos is an alternative to the standard approach of homoclinic intersections [12].

The study of the above mentioned second-order variations leads to the Jacobi–Levi-Civita equation of geodesic spread [13]. This equation describes the evolution of a vector field ξ through which the separation between nearby geodesics can be measured. The equation, in local coordinates, reads

$$\frac{\nabla}{ds}\frac{\nabla}{ds}\xi^i + R^i_{jlk}\frac{dq^j}{ds}\xi^l\frac{dq^k}{ds} = 0 , \tag{9}$$

where $(\nabla\xi/ds)$ is the covariant derivative along a geodesic and is given by

$$\frac{\nabla\xi^i}{ds} = \frac{d\xi^i}{ds} + \Gamma^k_{jk}\frac{dx^j}{ds}\xi^k . \tag{10}$$

R^i_{jlk} are the components of the Riemann curvature tensor

$$R^i_{jlk} = \frac{\partial\Gamma^i_{jk}}{\partial q^l} - \frac{\partial\Gamma^i_{jl}}{\partial q^k} + \Gamma^m_{jk}\Gamma^i_{ml} - \Gamma^m_{jl}\Gamma^i_{mk} . \tag{11}$$

The trace $R_{jk} = R^i_{jik}$ is the Ricci tensor and the scalar $\mathcal{R} = g^{jk}R_{jk}$ is the scalar curvature of M.

Now, assume that the configuration space of a mechanical system described by (2) is equipped with the Jacobi metric (6). The canonical connection coefficients are $\Gamma^h_{ij} = \frac{1}{2}W^{-1}\delta^{hm}(\partial_i W\delta_{jm} + \partial_j W\delta_{mi} - \partial_m W\delta_{ij})$, so by (10) and (11) we can easily compute the mathematical objects entering (9). In principle, the complete form of (9) should be used to study the stability properties of dynamics. In analogy with Lyapunov characteristic exponents, $\mathcal{N}$ new instability exponents could be defined by averaging, along a trajectory, the eigenvalues of the matrix $\mathcal{Q}^i_j = R^i_{ljk}\dot{q}^l\dot{q}^k$. Here a practical difficulty arises due to the large number of independent components of the Riemann tensor—$O(\mathcal{N}^4)$—without taking into account symmetries. It is evident that a numerical treatment of such a problem is likely to be rather cumbersome with a few tens of degrees of freedom. Thus, in a first approach, it is reasonable to seek an approximate form of (9) that might be more handy.

The first and most natural idea is to replace the system of $\mathcal{N}$ evolution equations for $\xi^1, \ldots, \xi^{\mathcal{N}}$—given by (9)—with a single scalar equation describing the evolution of the norm of the separation vector. Though in this way some information will be lost, knowing the evolution of the distance between two nearby geodesics is sufficient to describe their stability or their degree of instability.

To this purpose, let us multiply both sides of (9) by ξ to obtain

$$\langle \nabla^2_{\dot\gamma}\xi, \xi\rangle = -\langle R(\xi,\dot\gamma)\dot\gamma, \xi\rangle , \tag{12}$$

where $\nabla_{\dot\gamma}$ stands for the covariant derivative (10) and the angular brackets stand for scalar product. By standard algebraic manipulation of (12) one finds [14]

$$\frac{1}{2}\frac{d^2\|\xi\|^2}{ds^2} + \left[R_{ijkl}\mu^i\frac{dq^j}{ds}\mu^k\frac{dq^l}{ds}\right]\|\xi\|^2 - \left|\left|\frac{\nabla\xi}{ds}\right|\right|^2 = 0 , \tag{13}$$

where $\mu^i = \xi^i/\|\xi\|$ are the components of the unit vector codirectional with ξ. In order to work out a scalar equation for $\|\xi\|^2$ in closed form, we must make two approximations. First, we use the inequality

$$\left|\left|\frac{\nabla\xi}{ds}\right|\right|^2 \geq \left[\frac{d}{ds}\|\xi\|\right]^2 \tag{14}$$

to replace the last term in (13). Without loss of meaningful information we can choose as the initial condition for ξ a suitable eigendirection of the curvature matrix $\mathcal{Q}^i_j$. In such a case it can be shown [15] that Eq. (14) holds true with the sign of equality. Second, we need to replace $R_{ijkl}\mu^i\dot{q}^j\mu^k\dot{q}^l$ with something independent of μ (or, equivalently, ξ). To this purpose, we recognize that this quantity is just the sectional curvature $K^{(2)}$ associated with the plane spanned by ξ and $d\mathbf{q}/ds$. Of course, such a curvature depends upon the particular choice of ξ and $d\mathbf{q}/ds$ at a given point of M and still requires the knowledge of the evolution of ξ^i (or, equivalently, μ^i). Thus (13) is useless unless we can replace $K^{(2)}(\xi, d\mathbf{q}/ds)$ with a quantity independent of ξ. The ideal situation for such a replacement would be that of a manifold with constant curvature; in fact, in this case Schur's theorem [16] implies that all the sectional curvatures are independent of the orientation of the two-plane chosen and are equal to a common value independent of the point of the manifold.

Abstract ergodic theory mainly deals with this kind of manifold (assumed to be of negative constant curvature), whereas the configuration space manifolds associated with Hamiltonian flows of physical interest are in general neither of constant nor of negative curvature; on the contrary, curvature is wildly fluctuating along any geodesic [1,2]. However, if random initial conditions are considered, then it is found that curvature oscillates around a well-defined mean value. Loosely speaking, this suggests that a suitable "coarse graining" of the ambient manifold will make it look like a constant curvature manifold. So we can apply Schur's theorem to the coarse grained manifold in order to replace $K^{(2)}(\xi, d\mathbf{q}/ds)$ with a fraction of the average scalar or Ricci curvature. This is a first approximation in which fluctuations are neglected.

We shall see in the following that neglecting fluctuations has major consequences on the completeness of the geometric description of chaos. Let us refer to these fluctuations as "small scale fluctuations."

An immediate consequence of these small scale fluctuations is that there are two different possible replacements for the average of $K^{(2)}(\xi, d\mathbf{q}/ds)$ that would give the same result only in the case of true constant curvature manifolds. In fact, denote by $\xi_{(a)}$ and $(d\mathbf{q}/ds)_{(b)}$, $a,b = 1, \ldots, \mathcal{N}$, an arbitrary couple of mutually orthogonal vectors (there are $\mathcal{N}$ independent choices for each vector); then the sectional curvature relative to the plane spanned by $\xi_{(a)}$ and $(d\mathbf{q}/ds)_{(b)}$ is

$$K^{(2)}_{ab}\left[\xi,\frac{d\mathbf{q}}{ds}\right]\|\xi\|^2=R_{ijkl}\xi^i_{(a)}\left[\frac{dq^j}{ds}\right]_{(b)}\xi^k_{(a)}\left[\frac{dq^l}{ds}\right]_{(b)}, \tag{15}$$

where we have used $\|d\mathbf{q}/ds\|=1$; a well known result of Riemannian geometry [17] states that

$$\sum_{a,b}^{1,\ldots,\mathcal{N}} K^{(2)}_{ab}=\mathcal{R}\ , \tag{16}$$

where $\mathcal{R}$ is the scalar curvature of the manifold. This means that $\mathcal{R}/\mathcal{N}(\mathcal{N}-1)$ is a measure of the average sectional two-dimensional curvature at any point of M. Hence the quantity in parentheses in (13) could be approximated by $\mathcal{R}/\mathcal{N}(\mathcal{N}-1)$. This amounts to considering a local average over a set of geodesics issuing from a given point in every independent direction and over all the separation vectors orthogonal to them.

However, there is another *less drastic* approximation to the original equation (13): let us consider a *given* geodesic issuing from any point of M, i.e., we keep $d\mathbf{q}/ds$ fixed at that point, and let us consider all the possible sectional curvatures obtained by varying only the separation vector ξ. In such a case the sum (16) is replaced by

$$\sum_{a}^{1,\ldots,\mathcal{N}} K^{(2)}_{a}=\sum_{a}^{1,\ldots,\mathcal{N}}\left[\frac{1}{\|\xi\|^2}\right]R_{ijkl}\xi^i_{(a)}\frac{dq^j}{ds}\xi^k_{(a)}\frac{dq^l}{ds}$$
$$=R_{nm}\frac{dq^n}{ds}\frac{dq^m}{ds}\ ; \tag{17}$$

the last quantity is the Ricci curvature $K_R(\dot{\mathbf{q}})$ along the direction $d\mathbf{q}/ds$ and R_{nm} is the Ricci tensor. This suggests that we replace with $K_R(\dot{\mathbf{q}})/\mathcal{N}$ the quantity in parentheses in (13). Finally we have

$$\frac{1}{2}\frac{d^2\|\xi\|^2}{ds^2}+\tilde{\chi}\|\xi\|^2-\left[\frac{d\|\xi\|}{ds}\right]^2=0\ , \tag{18}$$

where

$$\tilde{\chi}=\frac{1}{\mathcal{N}}K_R(\dot{\mathbf{q}})=\frac{1}{\mathcal{N}}R_{nm}\frac{dq^n}{ds}\frac{dq^m}{ds} \tag{19}$$

or

$$\tilde{\chi}=\mathcal{R}/\mathcal{N}(\mathcal{N}-1) \tag{20}$$

and where we have made use of (14) taken with the sign of equality.

Equation (18) is an approximate version of Eq. (13), but now it describes in closed form the evolution of the norm of the separation vector ξ. The way any given trajectory probes the curvature properties of the underlying manifold enters (18) through $\tilde{\chi}$ and in so doing determines the stability or instability of the dynamics described by the Newtonian equations (8). In practice one has to solve simultaneously the equations of motion (8) and the stability equation (18) rewritten in terms of the Newtonian (absolute) time t, that is,

$$\frac{d^2\zeta}{dt^2}-\frac{1}{W}\frac{dW}{dt}\frac{d\zeta}{dt}+2\chi\zeta-\frac{1}{2\zeta}\left[\frac{d\zeta}{dt}\right]^2=0\ , \tag{21}$$

where

$$\chi=\frac{1}{\mathcal{N}}R_{nm}\frac{dq^n}{dt}\frac{dq^m}{dt} \tag{22}$$

or

$$\chi=2\mathcal{R}(E-V)^2/\mathcal{N}(\mathcal{N}-1) \tag{23}$$

and where $\zeta=\|\xi\|^2$. The explicit expressions of (22) and (23) are obtained by computing the components of the Ricci tensor $R_{nm}=R^i_{nim}$, which are given by

$$R_{nm}=\left[\frac{\Delta V}{2(E-V)}+\frac{4-\mathcal{N}}{4(E-V)^2}(\nabla V)^2\right]\delta_{nm}$$
$$+\frac{\mathcal{N}-2}{2(E-V)}\frac{\partial^2 V}{\partial q^n\partial q^m}+\frac{3(\mathcal{N}-2)}{4(E-V)^2}\frac{\partial V}{\partial q^n}\frac{\partial V}{\partial q^m}\ , \tag{24}$$

and the scalar curvature $\mathcal{R}=R^n_n$ given by

$$\mathcal{R}=\mathcal{N}(\mathcal{N}-1)\left[\frac{\Delta V}{\mathcal{N}(E-V)^2}-\left[\frac{1}{4}-\frac{3}{2\mathcal{N}}\right]\frac{(\nabla V)^2}{(E-V)^3}\right]\ . \tag{25}$$

Δ and ∇ stand for the Euclidean Laplacian and gradient, respectively.

By introducing standard transformations, Eq. (21) is transformed into (details are found in Ref. [1])

$$\frac{d^2X}{dt^2}-\frac{\dot{W}(t)}{W(t)}\frac{dX}{dt}+\chi(t)X=0 \tag{26}$$

and finally cast in the form

$$\frac{d^2Y}{dt^2}+Q(t)Y=0\ , \tag{27}$$

where

$$Q(t)=\chi(t)-\frac{1}{4}\left[\frac{\dot{W}}{W}\right]^2+\frac{1}{2}\frac{d}{dt}\left[\frac{\dot{W}}{W}\right]\ . \tag{28}$$

Equation (27) is in the form of a Hill equation. An exponential growth of $Y(t)$ implies an exponential growth of $X(t)$ and hence of $\zeta(t)$; a bounded evolution of $Y(t)$ implies a bounded evolution of $X(t)$ and hence of $\zeta(t)$.

Let us now notice that (a) $Q<0$ is a *sufficient* condition to get an exponential growth of $\zeta(t)$, thus to make chaos, and (b) $Q>0$ is a *necessary* condition for $\zeta(t)$ to remain bounded, thus for regular behavior. The latter item deserves particular attention. In fact, $Q>0$ is not *sufficient* to ensure the dynamical stability of nearby trajectories, because another mechanism, *parametric resonance,* is generally at work to make chaos also when $Q>0$, provided that Q fluctuates in a suitable manner. In other words, the bumpiness of the manifold (M,g_J) can be an effective source of exponential instability of nearby geodesics—thus of chaos—even in the presence of positive scalar or Ricci curvature. It is worth mentioning here that the generic situation of Hamiltonian flows of physical interest, i.e., those with bounding poten-

tials, parametric resonance appears as the largely predominant source of chaos [1,2,18]. Self-gravitating systems are in a very curious and instructive situation: in spite of the almost everywhere negative scalar curvature, chaos appears to stem mainly from the wildly oscillating behavior of $Q(t)$ through parametric instability, as shown in Sec. III.

However, the following two points should be clearly kept in mind: (i) the replacements of $R_{ijkl}\mu^i\dot{q}^j\mu^k\dot{q}^l$ in (13) either with $\mathcal{R}/\mathcal{N}(\mathcal{N}-1)$ or with $K_R(\dot{\mathbf{q}})/\mathcal{N}$ are not exact and (ii) by simple inspection of (26), it is well evident that the stability of its solutions is not entirely controlled by χ. In fact, the sign of the coefficient of dX/dt is not definite; thus the second term of (26) can alternatively act as a damping or an "antidamping" and a complete account of all the possible combined effects of the second and third terms of (26) is given by (27) and (28). $Q(t)$ instead of $\chi(t)$ is the meaningful quantity for chaos.

Let us now work out the explicit expressions of $Q(t)$ for both replacements of $\chi(t)$ with scalar or Ricci curvature and denote them respectively by $Q_S(t)$ and $Q_R(t)$. From (22) and (24) the Ricci curvature is easily found to be

$$\frac{1}{\mathcal{N}}K_R(\dot{\mathbf{q}})=\frac{\Delta V}{\mathcal{N}}+\frac{(\nabla V)^2}{\mathcal{N}(E-V)}+\frac{3(\mathcal{N}-2)}{4\mathcal{N}(E-V)^2}\left[\frac{dV}{dt}\right]^2+\frac{\mathcal{N}-2}{2\mathcal{N}(E-V)}\left[\frac{d^2V}{dt^2}\right]. \tag{29}$$

Combining (28) and (29) one gets

$$Q_R(t)=\frac{\Delta V}{\mathcal{N}}+\frac{(\nabla V)^2}{\mathcal{N}(E-V)}-\frac{3}{2\mathcal{N}(E-V)^2}\left[\frac{dV}{dt}\right]^2-\frac{1}{\mathcal{N}(E-V)}\left[\frac{d^2V}{dt^2}\right] \tag{30}$$

and from (23), (25), and (28)

$$Q_S(t)=2\frac{\Delta V}{\mathcal{N}}+\left[-\frac{1}{2}+\frac{3}{\mathcal{N}}\right]\frac{(\nabla V)^2}{(E-V)}-\frac{3}{4(E-V)^2}\left[\frac{dV}{dt}\right]^2-\frac{1}{2(E-V)}\left[\frac{d^2V}{dt^2}\right]. \tag{31}$$

It is quite natural to define the following geometric indicators of chaos (GICs) associated with Q_R and Q_S:

$$\overline{\Lambda}_R^t=\frac{1}{t}\int_0^t dt'[-Q_R^{(-)}(t')]^{1/2}, \tag{32}$$

$$\overline{\Lambda}_S^t=\frac{1}{t}\int_0^t dt'[-Q_S^{(-)}(t')]^{1/2}, \tag{33}$$

where by $Q_{R,S}^{(-)}$ it is meant $Q_{R,S}<0$. Similar quantities have been defined in [1]; however, the present definition is certainly more correct. These quantities, though this is mainly true for $\overline{\Lambda}_R$, are capable of qualitatively reproducing some important feature displayed by Lyapunov exponents [1] and we can attribute the quantitative discrepancies (the high energy scaling law) to the previous incomplete definition. Anyway, due to the crude elimination of small scale curvature fluctuations, the GICs convey only limited information about the source of chaos and its strength, as will be shown in Sec. III.

As we have already noticed, dealing only with sign definiteness of scalar or Ricci curvature is incorrect because in so doing one lacks the information given by the second term of Eq. (26). This term arises from the nonaffine time parametrization of the arc length of the configuration space manifold equipped with Jacobi metric, which means that the velocity along the geodesics is not constant. Here we have another nontrivial difference with abstract geodesic flows of ergodic theory, such as Anosov flows, which are defined on the unitary tangent bundle of a Riemannian manifold, which means that geodesics are spanned at constant velocity. This is a warning about naively borrowing tools from abstract ergodic theory. At this point any further progress requires the aid of computer simulations.

III. GRAVITATIONAL N-BODY SYSTEMS

Let us now focus our attention on the gravitational N-body problem. Krylov's original intuitions about the connection between phase space mixing and exponential instability of the dynamics have recently suggested a new approach to the description of relaxation and mixing of N gravitationally interacting particles [7–10].

In Ref. [7] it is claimed that the negativity of the average curvature of configuration space is a sufficient condition for an exponential divergence of the geodesics and thus a condition for a self-gravitating system to be mixing on a collective relaxation time scale related to the average curvature. Using the same approach, it has been argued elsewhere [10] that, owing to the fact that the average sectional curvature can actually be positive somewhere in the configuration space, one cannot conclude anything rigorously about the mixing properties of the system. Nevertheless, if the regions where the curvature is nonnegative are very small, one could speak of chaotic or mixing behavior. This analysis has established that the probability that a random perturbation of a random geodesic experiences a positive curvature decreases exponentially to zero as $N\rightarrow\infty$, suggesting that at least for short times, large systems should have a strongly chaotic behavior.

In the cited works on this subject, the detailed derivation given in Sec. II of a stability equation is lacking and only generic discussions about the negativity of scalar curvature have been proposed. In the following, we show that our more careful analysis of the geometric description of chaos, when applied to the self-gravitating N-body system, yields a completely new insight in the problem. Besides, the validity limits and the present difficulties of the geometric approach are also clearly assessed. In any case, the relevance and implications attributed to the

negativity of scalar curvature must be dropped when nonconstant curvature manifolds are involved.

We consider the gravitational N-body system described by the Hamiltonian

$$H=\sum_{i=1}^{N}\frac{1}{2m_i}(p_{xi}^2+p_{yi}^2+p_{zi}^2)-\sum_{i<j}G\frac{m_i m_j}{\mathbf{r}_{ij}}\ , \tag{34}$$

where $\mathbf{r}_{ij}^2=(x_i-x_j)^2+(y_i-y_j)^2+(z_i-z_j)^2$. In the above quoted papers, it is argued that for the Hamiltonian (34), ΔV can be neglected. In fact, by computing the Green's function for Poisson equation one gets [7]

$$\Delta_{\mathbf{r}}\left[\frac{1}{|\mathbf{r}-\mathbf{r}_0|}\right]=-4\pi\delta(|\mathbf{r}-\mathbf{r}_0|)\ , \tag{35}$$

where, using

$$V=-G\sum_{i<j}\frac{m_i m_j}{\mathbf{r}_{ij}} \tag{36}$$

and assuming that binary collisions are rare events, we get

$$\Delta V=4\pi G\sum_{i<j}m_i m_j\delta(|\mathbf{r}_i-\mathbf{r}_j|)\simeq 0\ . \tag{37}$$

Applied to Eq. (23), with the aid of (25), this gives

$$\chi=2\mathcal{R}\frac{(E-V)^2}{\mathcal{N}(\mathcal{N}-1)}\simeq -2\left[\frac{1}{4}-\frac{3}{2\mathcal{N}}\right]\frac{(\nabla V)^2}{(E-V)}$$
$$\underset{\text{large}\mathcal{N}}{\sim}-\frac{1}{2}\frac{(\nabla V)^2}{(E-V)}<0\ . \tag{38}$$

Hence one could be tempted to conclude that a large collection of bodies interacting gravitationally is always strongly chaotic and that the dynamical instability time scale is given by the square root of $2W/(\nabla V)^2$.

A. Numerical simulations

We have numerically followed the dynamics of N gravitationally interacting bodies together with the time evolution of $Y(t)$ obeying Eq. (27) and eventually providing the behavior of the geodesic separation vector norm ξ. We chose for $\chi(t)$ in Eq. (28) the Ricci curvature per degree of freedom according to the definition in (22) explicitly given by (29).

In view of the kind of information that we want to get from our numerical simulations, we have considered sufficient the use of either $N=10$ or 100 point masses. Though such numbers might seem exceedingly small with respect to those of current N-body simulations, they are at variance adequate for our purely theoretical study.

The $6N$ first-order Hamilton equations of motion, derived from (34), have been numerically integrated without any softening of the potential and by means of a second-order bilateral symplectic algorithm [2,19], which explicitly reads as

$$\begin{aligned}
&\tilde{q}_i=q_i(t)\ ,\\
&\tilde{p}_i=p_i(t)-\frac{1}{2}\Delta t\frac{\partial}{\partial\tilde{q}_i}V(\tilde{\mathbf{q}})\ ,\\
&q_i(t+\Delta t)=\tilde{q}_i+\Delta t\tilde{p}_i\ ,\\
&p_i(t+\Delta t)=\tilde{p}_i-\frac{1}{2}\Delta t\frac{\partial}{\partial q_i}V(\mathbf{q}(t+\Delta t))\ ,\\
&\hat{p}_i=p_i(t+\Delta t)\ ,\\
&\hat{q}_i=q_i(t+\Delta t)+\tfrac{1}{2}\Delta t\hat{p}_i\ ,\\
&p_i(t+2\Delta t)=\hat{p}_i-\Delta t\frac{\partial}{\partial\hat{q}_i}V(\hat{q})\ ,\\
&q_i(t+2\Delta t)=\hat{q}_i+\tfrac{1}{2}\Delta t p_i(t+2\Delta t)\ .
\end{aligned} \tag{39}$$

In spite of its simplicity, this scheme is precise and efficient. Moreover, being symplectic, it ensures a faithful local representation of a Hamiltonian flow.

We work with a system of units in which $G=1$ and all the masses are equal to the unit mass; thus $m_i=1$ $(i=1,\ldots,N)$. The initial conditions were chosen as follows. The spatial coordinates of each point mass have been selected at random in an initially given cubic volume with a uniform distribution. Also random initial velocities have been considered with a Gaussian distribution of their components. The variance of the velocity distribution was such that the expectation value of the kinetic energy fulfilled the virial condition $2\langle T\rangle=V$.

At given N, we have always worked with the same random initial condition and in order to change the total energy of the system we have rescaled the positions and the velocities. This fact ensures the homogeneity of the samples at different energies and rules out any possible doubt about the role of the initial conditions and possibly of an insufficient integration time of the dynamics in the observed phenomenology. Anyway, we have also checked the robustness of our results with respect to different choices of the initial conditions.

The numerical integration has been performed without any spatial restriction to the trajectories of the masses which are allowed—if it is the case—to escape up to infinity. Though in principle each point mass could evaporate, we never observed such an effect during our numerical simulations (with few bodies the high velocity tail of the distribution function is rarely populated). This practically means that the phase trajectories remained confined in some compact subspace of (M,g_J), so we were not actually confronted with the problem of noncompactness of the manifold (M,g_J) associated with the Hamiltonian (34). Noncompactness is just due to the possibility of producing unbound particles. If no point mass evaporates during an integration time much longer than the measured instability time, then one is allowed to speak of chaos whenever the dynamics is unstable.

Along any phase trajectory so obtained, we computed the different geometric quantities of interest and the GICs $\overline{\Lambda}_S^t$ and $\overline{\Lambda}_R^t$. The simultaneous integration of Eq. (27) along a trajectory provides another quantitative measure of the degree of chaos: the rate of the average ex-

ponential growth of $Y(t)$. This takes into account also parametric instability. Let us now discuss this in more detail.

A typical numerical sampling of $\mathcal{R}$ is reported in Fig. 1(a) in the case of $N=10$ and of energy density $\epsilon=|E/N|=0.0564$. By varying N and ϵ similar results are found, i.e., $\mathcal{R}$ is always strongly varying. Thus the configuration space manifold is far from being of constant curvature and Schur's theorem cannot be applied to properly replace $K^{(2)}$ with $\mathcal{R}/\mathcal{N}(\mathcal{N}-1)$. Besides, though the majority of values assumed by $\mathcal{R}(t)$ are negative, the corresponding values taken by $Q_S(t)$ are often also positive, as can be seen in Fig. 1(b). As a consequence, the solutions of (27) exponentially grow in time both because $Q_S(t)$ takes negative values and because the fluctuations of positive $Q_S(t)$ induce parametric resonance. The relevance of this phenomenon becomes more evident when the Ricci curvature is considered. Hereafter, unless otherwise stated, we will be concerned with quantities related with the Ricci curvature per degree of freedom $k_R(t)=K_R/\mathcal{N}=R_{mn}\dot{q}^m\dot{q}^n/\mathcal{N}$ because it corresponds to a lesser degree of approximation of (13) and because elsewhere it has been found to be more useful for the geometric description of chaos [1,2,18].

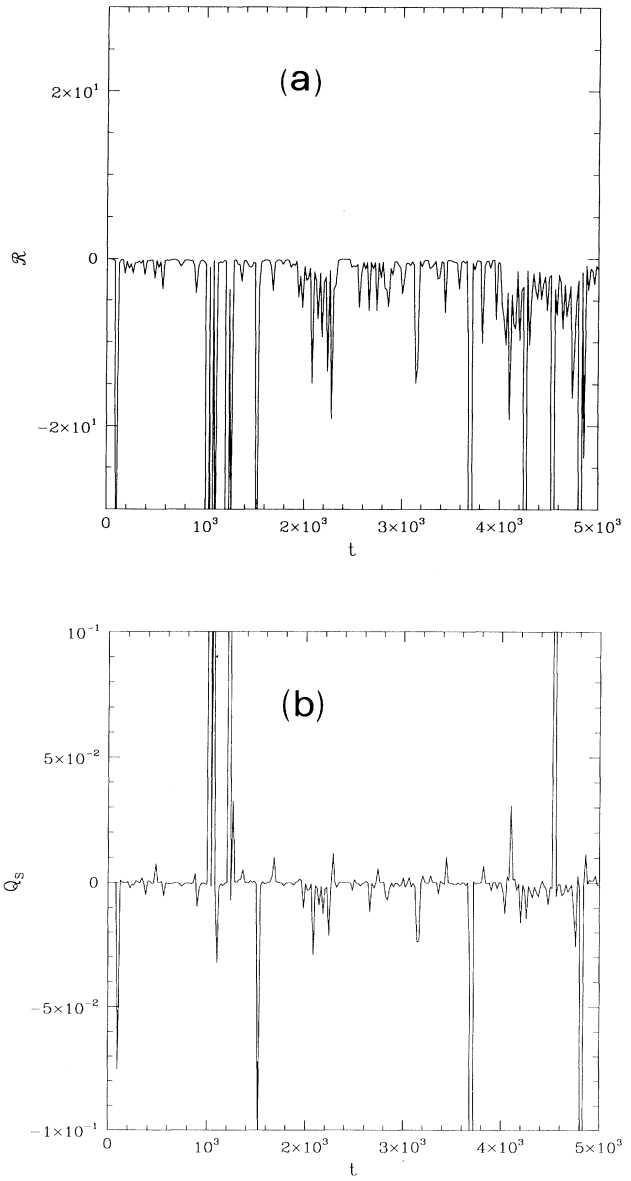

FIG. 1. (a) The scalar curvature $\mathcal{R}$ is plotted vs time for $N=10$ and energy density $\epsilon=0.0564$. (b) The time behavior of Q_S of Eq. (31) for the same parameters.

In Fig. 2(a) $k_R(t)$ is reported for the same example of Figs. 1(a) and 1(b). Also $k_R(t)$ is strongly fluctuating in time, but it takes also positive values and $Q_R(t)$ appears in Fig. 2(b) as almost always positive valued. As a matter of fact, the number of times that a phase trajectory encounters negative values of $Q_R(t)$ is a regularly increasing function of time [Fig. 2(c)], which makes meaningful the definition of $\bar{\Lambda}_R^t$ and possible its computation. In Fig. 2(b) $Q_R<0$ is seldom observed because of the sampling frequency and of the low probability of finding $Q_R<0$.

This latter circumstance makes parametric resonance—due to fluctuations of Q_R—the dominant mechanism of instability of the Hill equation (27) and thus of chaos. The existence of this effect is expected on the basis of a classical theory of stability whenever the frequency of a harmonic oscillator is modulated in time [20] and is proved here by numerical integration.

We have computed such solutions $Y(t)$ for different values of the energy density in the cases $N=10$ and 100. On the average, $Y(t)$ is exponentially growing and the growth rate is larger for the more bounded systems, as is reasonably expected. In Fig. 3(a) one such solution $Y(t)$ is reported for $N=10$ and for two different energy densities. At variance, if one keeps ϵ fixed and varies N, a surprising result shows up. The system seems to be more chaotic in the case of smaller N, which is against common physical sense. Figure 3(b) displays $Y(t)$ obtained at $\epsilon\simeq 0.06$ for $N=10$ (upper curve) and $N=100$ (lower curve).

We have estimated the exponential growth rates of the solutions of the Hill equation for several values of the energy density ϵ and for $N=10$ and 100. The resulting instability exponents λ_H are shown in Fig. 4. There are two noticeable features of these results: (i) λ_H displays a regular dependence upon ϵ both at $N=10$ and 100, precisely $\lambda_H(\epsilon)\sim\epsilon^{3/2}$, and (ii) the points $\lambda_H(\epsilon,N=10)$ define an experimental curve which is parallel to that defined by $\lambda_H(\epsilon,N=100)$; however, the former is displaced toward larger values. In other words, we have the confirmation that an increase in the number of degrees of freedom apparently results in a weakening of chaos.

On the basis of the comparison with the results obtained for other Hamiltonian systems, we claim that the weakening of chaos by increasing N is unreliable. In fact, for the Fermi-Pasta-Ulam model and for Lennard-Jones lattices [2,19], the computation of the Hill instability exponents gave the same effect with N, whereas measuring chaos through the largest Lyapunov exponent λ_1 shows an opposite tendency, i.e., an increase of chaos at larger

N and constant energy density. Thus we conclude that the weakening of chaos by increasing the number of degrees of freedom is likely to be a spurious effect of the approximations carried over Eq. (13).

The passage from Eq. (13) to Eq. (18) is a delicate point and in its present formulation causes the loss of some important information. Replacing the function $K^{(2)}$ by $k_R = K_R / \mathcal{N}$, we make an approximation in which the fluctuations of k_R and of Q_R tend to lower by increasing N. Now, owing to the fact that the fluctuations of Q_R play an important role in determining the degree of instability of the dynamics, the lowering of the fluctuation level due to the replacement of $K^{(2)}$ with k_R entails a weakening of parametric instability.

For the sake of a better approximation, we must retrieve in some way the fluctuations that have been discarded. Recently, this has been successfully done for the Fermi-Pasta-Ulam system [18] using Eisenhart's metric (see Sec. III B) and in the future it will be done for the self-gravitating systems.

The same kind of phenomena is clearly shown by $\overline{\Lambda}_R^t(\epsilon)$. In Fig. 5(a) some typical behaviors of $\overline{\Lambda}_R^t$ vs time and for two different values of energy density are reported for $N=10$. It is evident that the more bounded system is dynamically more unstable. Figure 5(b) displays $\overline{\Lambda}_R^t$ obtained at $\epsilon \simeq 0.06$ for $N=10$ (upper curve) and

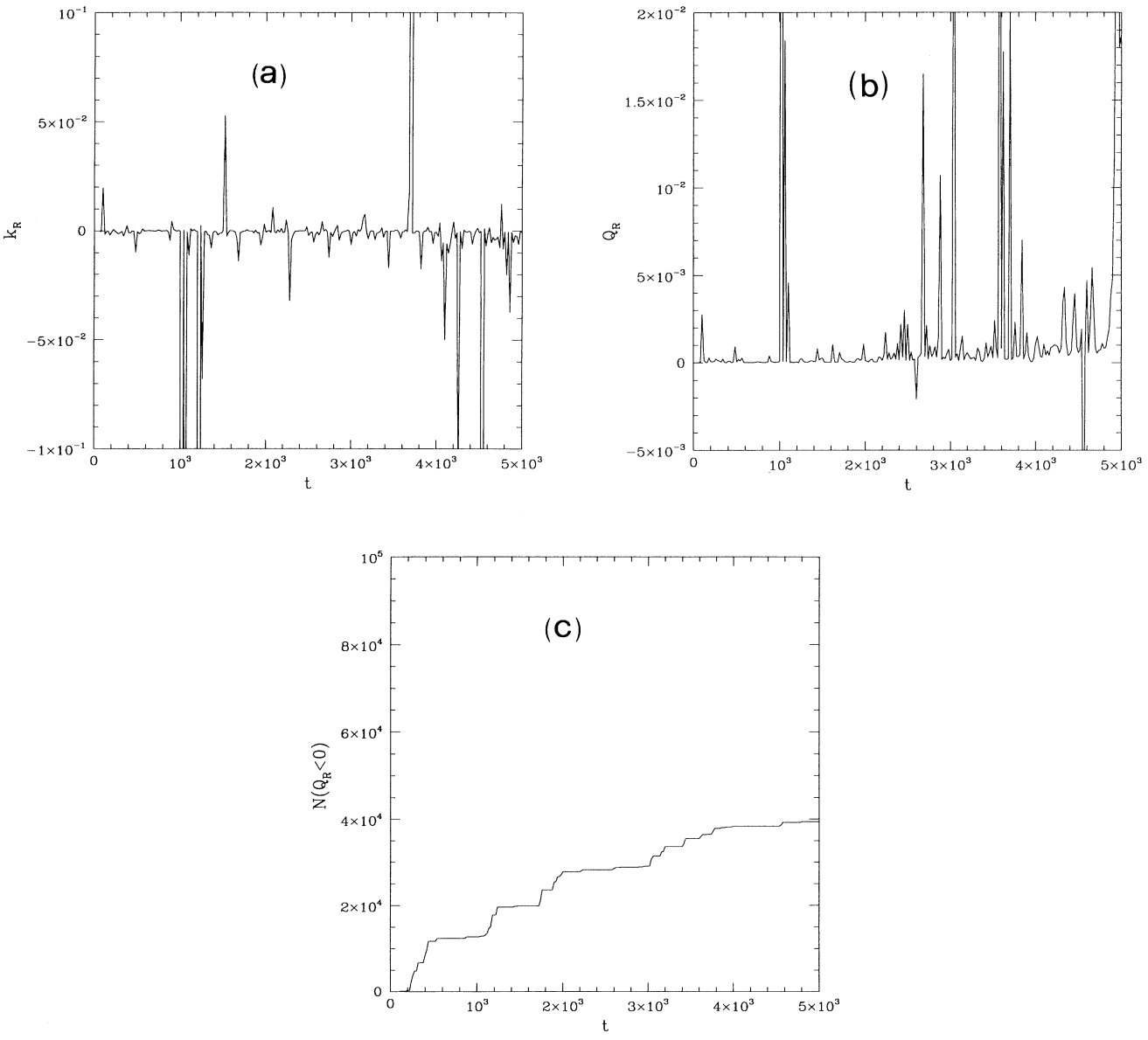

FIG. 2. (a) The time behavior of the Ricci curvature k_R per degree of freedom again for $N=10$ and $\epsilon=0.0564$. (b) The quantity Q_R of Eq. (30) is plotted vs time for the same values of N and energy density as in (a). (c) The number of times that $Q_R<0$ is plotted vs time. The parameters are the same as in Fig. 1.

$N=100$ (lower curve). The same effect already observed for λ_H shows up.

If we denote with Λ_R the mean value of $\overline{\Lambda}_R^t$ and compute it at different N and ϵ, we obtain the results plotted in Fig. 6. We observe again that $\Lambda_R \sim \epsilon^{3/2}$ and that the values at $N=10$ are systematically larger than the values at $N=100$.

If we make a comparison between λ_H and Λ_R at the same N and at each ϵ, we notice that $\lambda_H > \Lambda_R$. This is a very clear indication of the importance of parametric instability in the quantitative determination of the degree of chaos of the system. Moreover, the exponent 3/2 can be considered correct because it has been found for both $\lambda_H(\epsilon)$ and $\Lambda_R(\epsilon)$, independently of N.

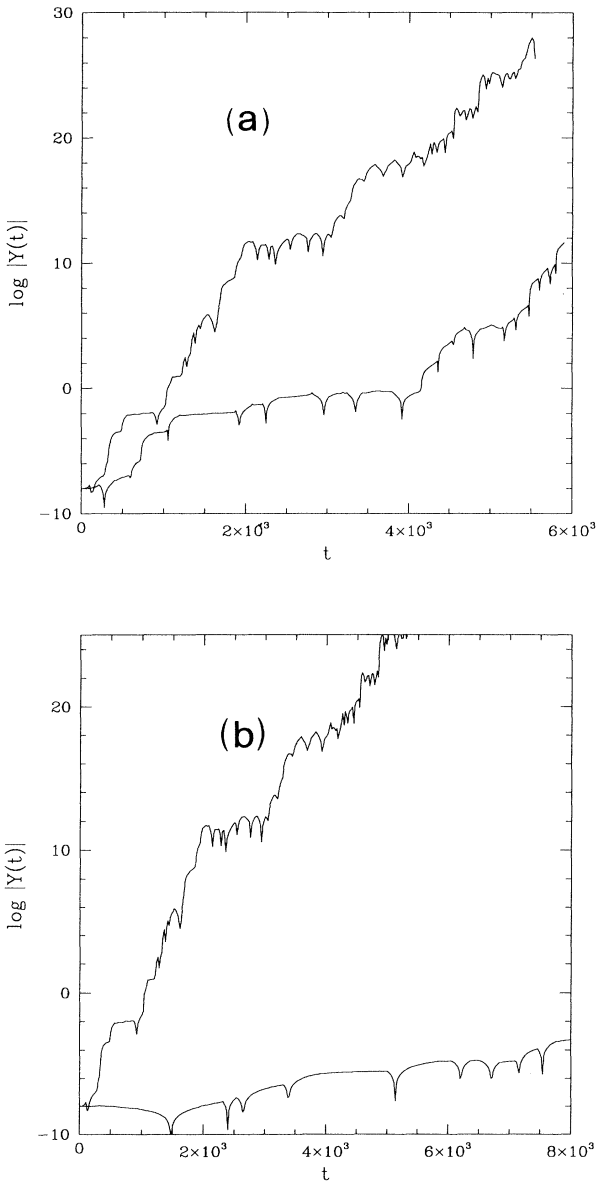

FIG. 3. (a) Typical solutions $Y(t)$ of the Hill equation (27) are plotted for $N=10$ and $\epsilon=0.0564$ (upper curve) and $\epsilon=0.0338$ (lower curve). (b) Typical solutions $Y(t)$ of the Hill equation (27) are plotted at $\epsilon \simeq 0.06$ for $N=10$ (upper curve) and $N=100$ (lower curve). (Logarithms are decimal.)

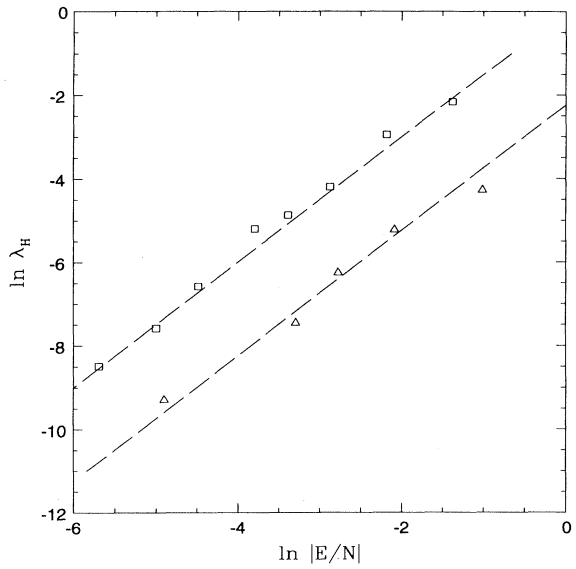

FIG. 4. The Hill instability exponent λ_H is plotted vs energy density for $N=10$ (squares) and $N=100$ (triangles). Dashed lines are references to power law $\epsilon^{3/2}$.

It is worth reporting here that also the quantity Λ_S, related to the scalar curvature, displays the same effect of weakening chaos by increasing N. In Fig. 7 $\overline{\Lambda}_S^t$ is plotted vs time; the computation has been performed at $\epsilon \simeq 0.06$ for $N=10$ and 100. Though the curve relative to $N=10$ has not yet reached an asymptotic value, it is clear that it remains well above the curve relative to $N=100$ by one order of magnitude.

We have verified that this is the case at any ϵ. This agrees with the above reported results found using Ricci curvature. It is not out of place mentioning that the averages of scalar-related quantities need a much longer computing time to converge to an asymptotic value. This is an additional reason to prefer the use of Ricci-related quantities. Anyway, we have a consistent analogy between the behavior of "Ricci-related" and "scalar-related" quantities. Besides, let us remark that the N dependence of the measured quantities is not simply deducible by pure inspection of their analytic expressions. In this context, numerical simulations reveal themselves as a powerful and inevitable tool for they yield autonomous information which is complementary to the analytic approach.

B. Lyapunov exponents for self-gravitating systems

Let us now briefly discuss the relationship between the above Riemannian description of chaos and Lyapunov characteristic exponents (LCEs). Details about this point can be found in [1] and [2]. The point naturally arises because the use of LCEs as detectors of chaos in numerical simulations is widespread; moreover LCEs are commonly

accepted as the closest indicators to the standard definition of chaos.

In order to tackle this point, we recall that the choice of the ambient manifold (M,g_J) is not unique. An interesting alternative is given by the enlarged configuration space time endowed with Eisenhart metric $(M\times\mathbb{R}\times\mathbb{R},g_E)$. This is the n-dimensional configuration space M $(q^1,\ldots,q^n\in M)$ with two additional coordinates: time $(q^0\in\mathbb{R})$ and something tightly related to Hamiltonian action $(q^{n+1}\in\mathbb{R})$.

This space is the set of all the possible configurations of a mechanical system at different and continuously varying times and actions. Time is a parameter in the Newtonian sense.

A simple but nontrivial metric g_E on this space was given by Eisenhart [21], who introduced the additional coordinate $q^{n+1}\in\mathbb{R}$ so that the time parametrization of the arc length becomes affine and the natural motions are obtained as geodesics of this metric. Eisenhart's arc length is written as

$$ds_E^2=a_{ij}dq^i dq^j-2V(q^a)(dq^0)^2+2dq^0dq^{n+1}\ . \qquad (40)$$

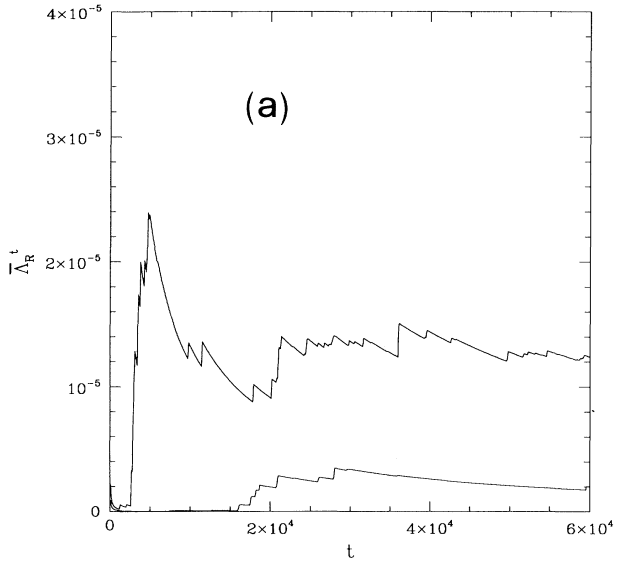

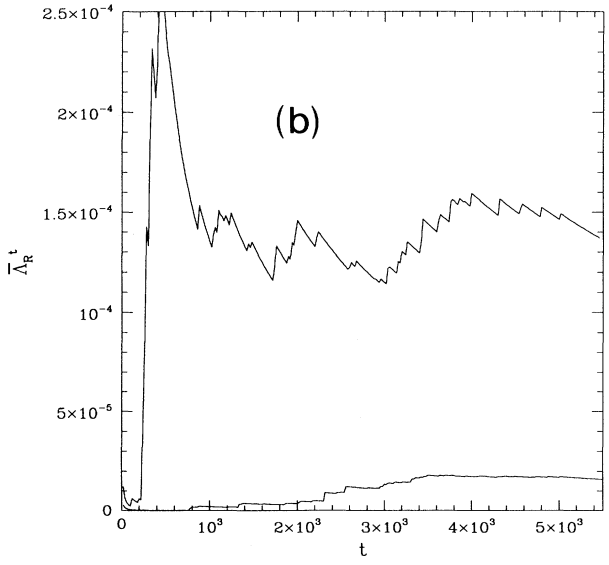

FIG. 5. (a) The quantity $\bar{\Lambda}_R^t$ is plotted for $N=10$ at $\epsilon=0.0113$ (upper curve) and $\epsilon=0.0034$ (lower curve). (b) The quantity $\bar{\Lambda}_R^t$ is plotted vs time at $\epsilon\simeq 0.06$ for $N=10$ (upper curve) and $N=100$ (lower curve).

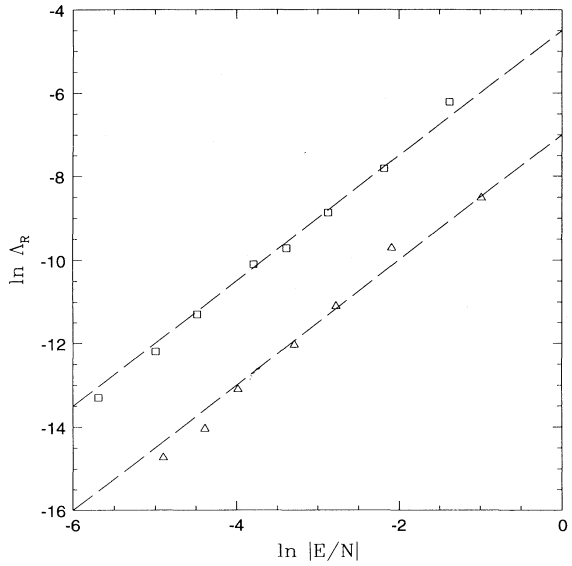

FIG. 6. The quantity Λ_R is plotted vs energy density for $N=10$ (squares) and $N=100$ (triangles). Dashed lines are references to power law $\epsilon^{3/2}$.

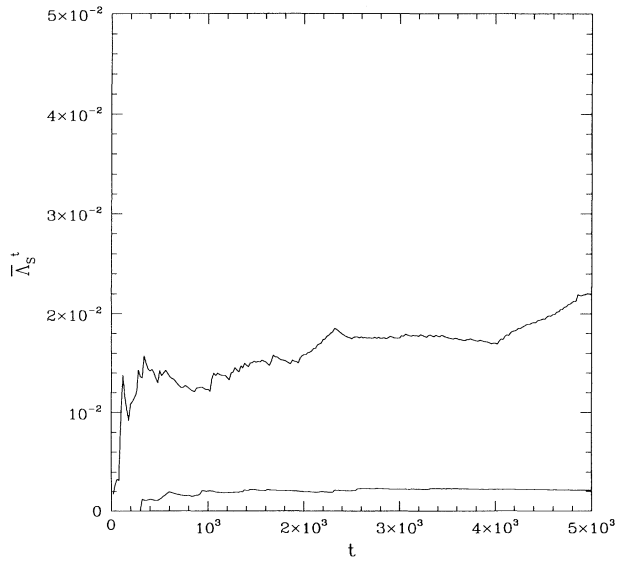

FIG. 7. The quantity $\bar{\Lambda}_S^t$ is plotted vs time at $\epsilon\simeq 0.06$ for $N=10$ (upper curve) and $N=100$ (lower curve).

It is possible to compute explicitly the function $q^{n+1}(t)$ as

$$q^{n+1}(t)=k^2t+C-\int_0^t dt\, L(q^a,\dot{q}^a)\ , \tag{41}$$

which shows why q^{n+1} is related to the action; k^2 and C are real constants.

The nonvanishing connection coefficients associated with g_E can be easily computed and for $a_{ij}=\delta_{ij}$ they are $\Gamma^i_{00}=\partial V/\partial q_i$ and $\Gamma^{n+1}_{0i}=-\partial V/\partial q^i$, so that the geodesic equations are

$$\frac{d^2q^i}{ds^2}+\Gamma^i_{00}(q^a)\frac{dq^0}{ds}\frac{dq^0}{ds}=0,\quad i=1,\ldots,n \tag{42}$$

$$\frac{d^2q^{n+1}}{ds^2}+\Gamma^{n+1}_{0i}(q^a)\frac{dq^0}{ds}\frac{dq^i}{ds}=0\ , \tag{43}$$

$$\frac{d^2q^0}{ds^2}=0\ ,$$

and since $ds_E^2=k^2dt^2$, one finds

$$\frac{d^2q^i}{dt^2}=-\frac{\partial V}{\partial q^i},\quad i=1,\ldots,n \tag{44}$$

$$\frac{d^2q^{n+1}}{dt^2}=\frac{\partial V}{\partial q^i}\frac{dq^i}{dt}=-\frac{dL}{dt}\ , \tag{45}$$

$$\frac{d^2q^0}{dt^2}=0\ .$$

The first n equations are obviously Newton's equations, the evolution equation for q^{n+1} is the differential version of (41), and the last equation states that $q^0=t$.

The only nonvanishing components of the Riemann tensor are

$$R_{0i0j}=\frac{\partial^2V}{\partial q^i\partial q^j}\ ; \tag{46}$$

hence we can compute the explicit expression of the Jacobi–Levi-Civita equation for this metric, finding that only $\xi^1,\ldots,\xi^n$ have a nontrivial evolution [2]. Equation (9) then becomes

$$\frac{d^2\xi^i}{dt^2}+\left[\frac{\partial^2V}{\partial q_i\partial q^j}\right]\xi^j=0,\quad i=1,\ldots,n\ , \tag{47}$$

which is the standard equation for the tangent dynamics and is used to compute numerical Lyapunov exponents according to a widespread algorithm [22]. It is commonplace that numerical LCEs are asymptotic quantities. This belief is based on the mathematical definition of *true* LCEs as eigenvalues of a limiting matrix of an infinite product of matrices [23]; the existence of such a finite limit is ensured by Oseledets' multiplicative ergodic theorem. However, there is no rigorous proof of the link between the standard numeric algorithm and Oseledets' theorem and true LCEs should be computed in a completely different way [1].

Having recognized the differential geometrical origin of (47), we can give an alternative interpretation of the meaning of the standard numerical algorithm and the instability exponents so computed are not at all asymptotic quantities. In other words, since the geodesics of $(M\times\mathbb{R}\times\mathbb{R},g_E)$ project on the natural motions in configuration space and since the tangent dynamics equation is derived from the JLC equation written for Eisenhart metric, when one computes LCEs by means of the standard algorithm, one uses Riemannian geometry without being aware of it. Obviously this is true also for the gravitational N-body systems, but, unfortunately, in this particular case we cannot use the scalar equation (21) because the Ricci curvature for the Eisenhart metric is $K_R=\nabla^2V(\mathbf{q})$ and after (37) $K_R=0$. In regard to the scalar curvature, one easily finds that it is $\mathcal{R}=0$ *identically* for any potential function V. This last circumstance shows once more that the scalar curvature conveys less information than the Ricci curvature. Thus only the full Eq. (47) can be used for self-gravitating systems.

In conclusion, while *true* LCEs, i.e., asymptotic quantities, might be ill defined in the case of gravitational N-body systems because of noncompactness of the ambient manifold, *numerical* LCEs are well defined and meaningful for any finite observational time scale. This provides a mathematical support to the concept of local Lyapunov exponents already used in Ref. [24]. Therefore, the stability properties of the dynamics of self-gravitating systems are correctly investigated by means of the simultaneous integration of the equations of motion and of Eq. (47) and the results are meaningful, provided that no mass evaporates during a time lapse much longer than the average instability time scale.

IV. CONCLUSIONS

In this paper we have discussed the consequences of the simplest approximations that can be performed on the Jacobi–Levi-Civita equation for geodesic spread when this equation is used to describe the intrinsic chaos of Hamiltonian dynamics. We have comparatively discussed the use of scalar and Ricci curvatures. We have investigated the origin of chaos in a collection of gravitationally interacting point masses with the aid of numeric simulations. One of the most interesting results of these simulations is that the degree of chaos of the system is not determined by the scalar curvature of configuration space, even if almost everywhere negative. This is due to the fact that the ambient manifold is not a constant curvature manifold, which implies that the relevant sectional curvature along a given geodesic is not simply given by a fraction of scalar curvature.

Besides, the nonaffine parametrization of the arc length with time, proper to the Jacobi metric, has another relevant consequence: neither scalar nor Ricci curvature determines the stability or instability of geodesics, which are rather determined by the curvature-related quantities Q_S and Q_R.

Between the curvature-related quantities, Q_R, related to the Ricci curvature, corresponds to a lesser degree of approximation and is shown to be preferable to Q_S, related to the scalar curvature. Using Q_R to describe chaos in a self-gravitating system entails a curious situation; even though the scalar curvature of the configuration space is

almost everywhere negative, chaos is mainly due to *parametric resonance* induced by the fluctuations of Q_R, which is only seldom negative. This is the big difference with geodesic flow of abstract ergodic theory for which the negativity of scalar curvature of the ambient manifold is necessary and sufficient for chaos and mixing.

Numerical simulations have shown that the reduction of the JLC equation to the "effective" form (18)—or equivalently (27)—causes an important loss of information for what concerns the N dependence of all the chaos indicators. Apparently the strength of chaos is reduced by increasing the number of particles at constant energy density ϵ. We have discussed why this paradoxical result is fake. In a future work we shall show how to solve this problem with an improved approximation.

On the other hand, we find that all the instability exponents—independently of N—exhibit the functional dependence $\epsilon^{3/2}$; therefore some meaningful information survives the above mentioned approximations. What is still lacking is some nontrivial normalization which will hopefully be found with the above mentioned improvements of (21).

Let us conclude with a few remarks pertaining to the particular system that we have investigated. The aim of our numerical computations is to help and to complement the theoretical analysis of Hamiltonian chaos from a Riemannian point of view. Therefore, our numerical experiments are conceived to meet this purpose, which has nothing to do with the aims of the usual N-body simulations in different contexts.

Finally, there is no evidence of the strong stochasticity threshold found in other models, i.e., of a transition between different dynamic regimes of weak and strong chaos revealed by a crossover in the ϵ dependence of the chaos indicators [1,2,25,26]. We could venture a guess that this is due to the absence of a minimum in the interaction potential and thus to the absence of a "harmonic limit" of the system at low energy density.

[1] M. Pettini, Phys. Rev. E **47**, 828 (1993).
[2] L. Casetti and M. Pettini, Phys. Rev. E **48**, 4320 (1993).
[3] N. S. Krylov, Ph.D. thesis, Leningrad Physical and Technical Institute, 1942 [reprinted in *Works on the Foundations of Statistical Physics* (Princeton University Press, Princeton, 1979)].
[4] Ya. B. Pesin, in *Dynamical Systems II,* edited by Ya. G. Sinai, Encyclopaedia of Mathematical Sciences Vol. 2 (Springer-Verlag, Berlin, 1989).
[5] M. C. Gutzwiller, J. Math. Phys. **18**, 806 (1977).
[6] A. Knauf, Commun. Math. Phys. **110**, 89 (1987).
[7] V. G. Gurzadyan and G. K. Savvidy, Astron. Astrophys. **160**, 203 (1986).
[8] H. E. Kandrup, Phys. Lett. A **140**, 97 (1989).
[9] H. E. Kandrup, Physica A **169**, 73 (1990).
[10] H. E. Kandrup, Astrophys. J. **364**, 420 (1990).
[11] M. Cerruti-Sola and M. Pettini (unpublished).
[12] J. Guckenheimer and P. Holmes, *Nonlinear Oscillations, Dynamical Systems, and Bifurcation of Vector Fields* (Springer-Verlag, New York, 1983).
[13] T. Levi-Civita, Ann. Math. **97**, 291 (1926).
[14] See, for example, E. T. Whittaker, *A Treatise on the Analytical Dynamics of Particles and Rigid Bodies* (Cambridge University Press, Cambridge, England, 1937), Chap. XV, p. 419.
[15] L. Casetti, C. Clementi, and M. Pettini (unpublished).
[16] M. P. Do Carmo, *Riemannian Geometry* (Birkhäuser, Boston, 1992).
[17] S. I. Goldberg, *Curvature and Homology* (Academic, New York, 1962).
[18] L. Casetti, R. Livi, and M. Pettini, Phys. Rev. Lett. (to be published).
[19] L. Casetti, Master thesis, University of Florence, 1993.
[20] A. H. Nayfeh and D. T. Mook, *Nonlinear Oscillations* (Wiley, New York, 1979).
[21] L. P. Eisenhart, Ann. Math. **30**, 591 (1929).
[22] G. Benettin, L. Galgani, and J.-M. Strelcyn, Phys. Rev. A **14**, 2338 (1976).
[23] V. I. Oseledets, Trans. Moscow Math. Soc. **19**, 197 (1968).
[24] G. D. Quinlan and S. Tremaine, Mon. Not. R. Acad. Soc. **259**, 505 (1992).
[25] M. Pettini and M. Landolfi, Phys. Rev. A **41**, 768 (1990).
[26] M. Pettini and M. Cerruti-Sola, Phys. Rev. A **44**, 975 (1991).